# THE UCLA/FNPL TIME RESOLVED UNDERDENSE PLASMA LENS EXPERIMENT[*]

M.C. Thompson[†], H. Badakov, J.B. Rosenzweig, G. Travish, UCLA, Los Angeles, CA, 90095, USA
H. Edwards, R. Fliller, G. M. Kazakevich, P. Piot, J. Santucci, FNAL, Batavia, Illinois, 60510, USA
J. Li, R. Tikhoplav, University of Rochester, Rochester, New York 14627, USA

## Abstract

A gaussian underdense plasma lens with peak density 5 x $10^{12}$ cm$^{-3}$ and a full width half maximum (FWHM) length of 2.2 cm has been used to focus a relativistic electron beam. This plasma lens has a focusing strength equivalent to a quadrupole magnet with a 150 T/m field gradient. The lens focused a 15 MeV, 16 nC electron beam with initial dimensions $\sigma_r = 500$ $\mu$m and $\sigma_z = 5$ mm onto an optical transition radiation (OTR) screen 2 cm downstream of the lens. The average transverse area of the plasma focused electron beam was typically demagnified by a factor of 22. The light from the OTR screen was imaged into a streak camera in order to directly measure the correlation between z and $\sigma_r$ within the beam.

## INTRODUCTION

Plasma lenses are of great interest to the accelerator physics community because they can theoretically provide radially symmetric focusing gradients on the order of 10 MT/m, which exceeds the strength of conventional quadrupole lens by several orders of magnitude [1]-[3]. Increasing focusing gradients to this level would greatly aid in achieving the small spot sizes and high luminosity necessary for future $e^+e^-$ colliders such as the planned International Linear Collider (ILC). Additionally, it has been shown that adiabatic plasma lenses can overcome the synchrotron-radiation limit on final focus spot size [4]. The underdense regime of plasma lens operation, in which the density of beam electrons $n_b$ is greater than half of the plasma density $n_p$, is considered the most advantageous for the focusing of electron beams in many scenarios [2, 4].

The most commonly considered regimes of plasma lens operation are the overdense ($n_b << n_p$) and underdense ($n_b > n_p/2$) regimes [3]. In the overdense case the plasma essentially cancels the beam space charge and allows it to focus under its magnetic self forces. Since the beam magnetic field depends on the beam current, which is generally not uniform over the length of the bunch, overdense lenses typically have significant abberations. In the underdense case the strong space charge of the electron beam ejects the plasma electrons entirely, leaving a uniform ion column. It can be shown that the radial focusing force of this ion column is given by

$$F_{radial} = -2\pi n_p e^2 r, \qquad (1)$$

where $e$ is the electron charge and $r$ is the radial distance from the axis. An underdense plasma lens is hence equivalent in strength to a quadrupole focusing magnet with a magnetic gradient of (3 x $10^{-11}$)$n_p$ T/m. A plasma lens with the relatively modest density of 5 x $10^{12}$ cm$^{-3}$ therefore has the strength of a 150 T/m quadrupole. State-of-the-art superconducting quadrupoles by comparison have maximum gradients on the order of 250 T/m. Plasma lenses also focus both transverse beam axes simultaneously. The drawback of plasma lens in either regime of operation is that only about 80 % of the beam is focused. Due to the finite time it takes for the plasma to react to the beam space charge, the head of the beam is not subject to the plasma focusing forces.

## EXPERIMENTAL METHODOLOGY

Our underdense plasma lens experiment, which evolved from earlier proposals [5, 6] and follows previous electron plasma lens work in other regimes [7]-[10], was conducted at the Fermilab NICADD Photoinjector Laboratory (FNPL) at FNAL. A schematic of the experiment is shown in Fig.1. A bulk column of plasma approximately 5 cm FWHM is produced using our pulsed argon discharge plasma source [11]. A slice of this static plasma column is selected using a translatable mask with a 1.25 cm wide slit. This arrangement allows the distance between the thin plasma lens column and the fixed OTR diagnostic screen to be varied without altering the OTR collection optics. Mea-
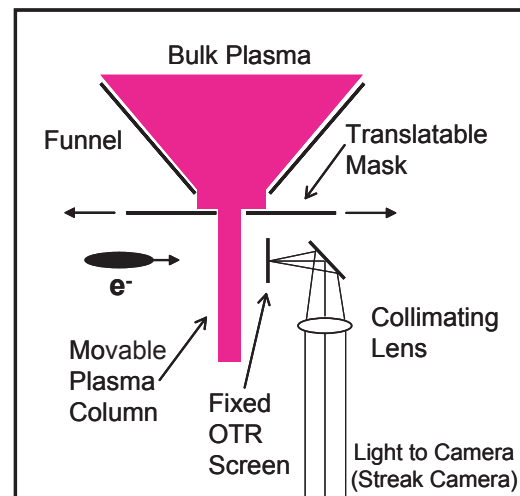


Figure 1: Schematic of the plasma lens apparatus.

[†] mct@physics.ucla.edu

Unfocused - 5 electron pulses



Focused - 1 electron pulse
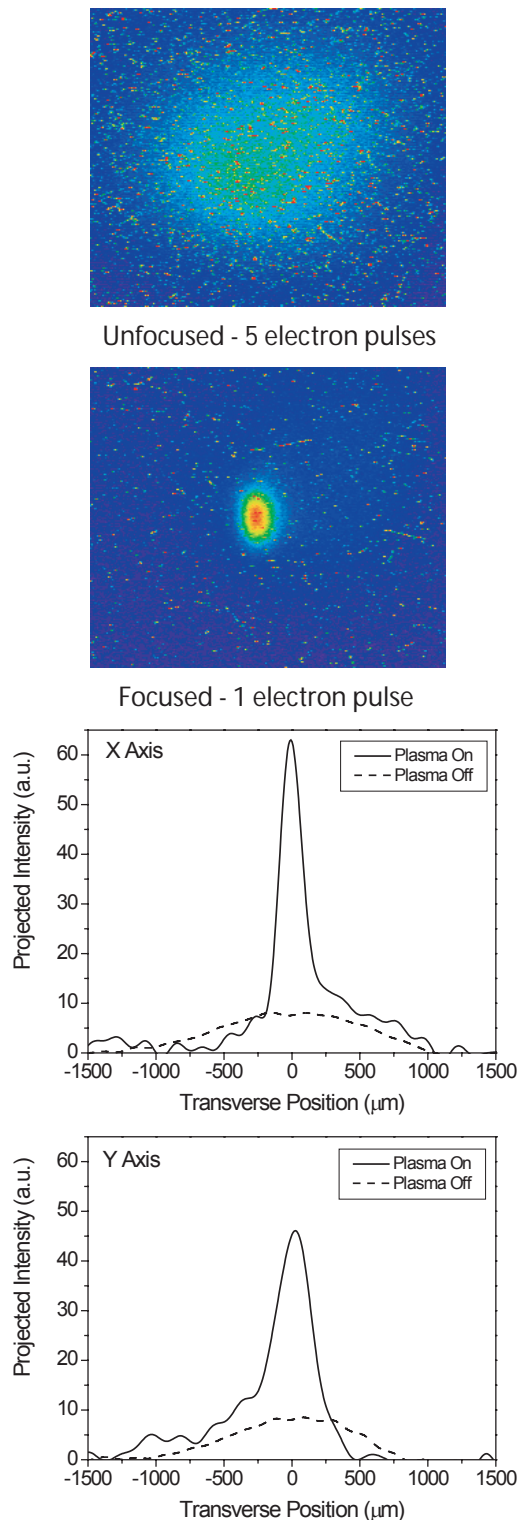




Figure 2: First Frame (Top): False color image of the unfocused electron beam spot, shown at five times normal intensity in order to provide sufficient image contrast, on the OTR screen after the plasma lens. Second Frame: False color image of the plasma focused electron beam spot on the OTR screen. Third and Fourth Frames: Plots of the image intensity of the above photographs (normalized to 1 electron pulse) in the x axis (third) and y axis (fourth).

surements have shown that the plasma lens column properties, listed in Table 1, vary only slightly as the mask is translated through the 1 cm region of interest. An in-vacuum, 160 mm focal length, 2 inch diameter lens provides point to parallel collimation of the OTR produced when the electron beam emerges from the back of a polished aluminum foil. The OTR is then transported either 30 cm to a conventional CCD camera with a 75 mm compound camera lens or 7 m to a streak camera where the light is imaged onto the streak slit using a single 280 mm focal length lens.

The electron beam for the experiment is provided by the FNPL electron accelerator. The FNPL accelerator is a 15 MeV electron linac [12] consisting of a normal conducting L-band RF gun with a cesium telluride photo-cathode and a 9-cell superconducting accelerating cavity. After acceleration, the electron beam is propagated at a tight focus through a $10\mu m$ thick aluminum vacuum foil, used the isolate the plasma experiment vacuum from the rest of the beam line, and refocused into the plasma lens experiment. The beam parameters delivered to the plasma lens are listed in Table 1.

## UNDERDENSE PLASMA FOCUSING

Three distinct series of measurements were made during this experiment: time integrated measurements of round focused spots, time resolved measurements of round focused spots, and time integrated measurements of focused beams with ratios of x dimension to y dimension of up to 1:5.

Fig. 2 shows the effect of plasma focusing on the electron beam spot size as observed with the conventional CCD camera. Note that the focused image shows the focused core of the beam and the unfocused head overlapped on top of each other; at a focal length of 1.9 cm. The unfocused beam is nearly round with x FWHM = 1200 $\mu$m and y FWHM = 1100 $\mu$m. The underdense plasma lens focuses this beam down to x FWHM = 200 $\mu$m and y FWHM = 300 $\mu$m which is a demagnification of 6 in x and 3.66 in y. The average transverse area of the beam is consequently reduced by a factor of 22. If the difference between head and core focusing are ignored this area reduction would equate to a boost in the peak beam density from 5 x $10^{12}$ cm$^{-3}$ in the unfocused case to 1 x $10^{14}$ cm$^{-3}$ in the focused case. In reality, the peak density of the focused core is even higher.

A series of time resolved measurements of the plasma

Table 1: Experimental Parameters

| Peak Plasma Density | 5 x $10^{12}$ cm$^{-3}$ |
|---|---|
| Plasma Thickness ($\sigma_p$) | 9.6 mm |
| Beam Charge | 16 nC |
| Beam Duration ($\sigma_t$) | 18 ps |
| Initial Beam Radius ($\sigma_r$) | 500 $\mu$m |
| Beam Emittance ($\varepsilon_n$) | 37 mm-mrad |
| Peak Beam Density | 5 x $10^{12}$ cm$^{-3}$ |
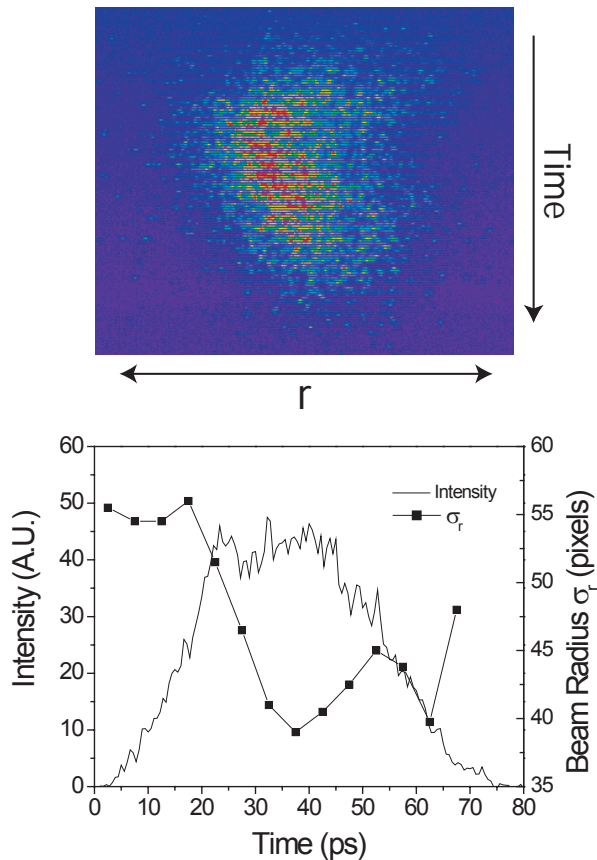
Figure 3: A false color streak camera image of the plasma focused beam (top) with initial analysis of the image (bottom).

focusing were made by imaging the beam OTR light onto the slit of a Hamamatsu series C5680 streak camera. An example of one the images recorded on the streak camera, along with an analysis of that shot, is shown in Fig. 3. As expected, the intensity profile of the focused beam in the time domain remains roughly gaussian while the beam is radially larger at the head than in the middle or tail. Width measurements were made by examining 5 ps wide swaths of the beam. The time resolution of the streak camera had previously been measured to be below 2 ps. While the time domain behavior of the plasma focusing is in general agreement with theoretical predictions, the raw data does not have as large a change between head and tail diameter as expected from either theory or the time integrated measurements. This apparent lack of transverse resolution seems to originate from limitations in the performance of our OTR light transport and may result from slight optics misalignments, the large angles inherent in such a strongly focused beam, and other effects.

Fig. 4 shows an example of a time integrated measurement of a beam with a 1:3.4 aspect ratio between x and y dimesions. Beams with x:y aspect ratios of up to about 1:5 were examined. The motivation behind these measurements is the desire to understand how the dynamics of un-
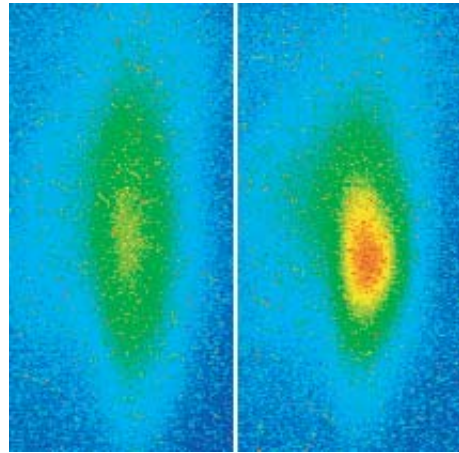


Figure 4: False color images of a beam with an initial 1:3.4 aspect ratio. At left the plasma is off, at right the plasma is on. Both images show the same number of beam pulses.

derdense plasma focusing change as the beam aspect ratio increases. The development of such an understanding is vital if underdense lenses are to be applied in a ILC context where aspect beam ratios at the interaction point are 1:100.

We have measured extreme demagnification of a high brightness electron beam by a strong underdense plasma lens. While some of the finer aspects of our measurements, such as the slight asymmetry in x and y focusing shown in Fig. 2 and the limited transverse resolution of the streak camera images, require further analysis to interpret, the general behavior of the plasma lens matches our theoretical expectations very well. A full analysis of this underdense plasma lens experiment will be reported elsewhere [13].

## ACKNOWLEDGEMENTS

## REFERENCES

[1] P. Chen. *Part. Accel.*, **20**, 171 (1987).

[2] P. Chen, *et al.*, *Phys. Rev. D*, **40**, 923 (1989).

[3] J. Su, *et al.*, *Phys. Rev. A*, **41**, 3321 (1990).

[4] P. Chen, *et al.*, *Phys. Rev. Lett.*, **64**, 1231 (1990).

[5] H. Suk, *et al.*, In *Proc. PAC 1999*, 3708 (1999).

[6] M. C. Thompson, *et al.*, In *Proc. PAC 2001*, 4014 (2001).

[7] H. Nakanishi, *et al.*, *Phys. Rev. Lett.*, **66**, 1870 (1991).

[8] G. Hairapetian, *et al.*, *Phys. Rev. Lett.*, **72**, 2403 (1994).

[9] R. Govil, *et al.*, *Phys. Rev. Lett.*, **83**, 3202 (1999).

[10] P. R. Bolton, *et al.*, Int. J. Mod. Phys. A **18**, 2843 (2003).

[11] M. C. Thompson, *et al.*, *Rev. Sci. Instr.*, **76**, 013303 (2005).

[12] J.-P. Carneiro, *et al.*, In *Proc. PAC 1999*, 2027 (1999).

[13] M. C. Thompson, *et al.*, *Phys. Rev. Lett.*, (to be submitted).